Heliyon 10 (2024) e28641

Contents lists available at ScienceDirect

Heliyon

journal homepage: www.cell.com/heliyon

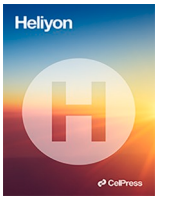

Research article

Environmentally safe biopolymer-clay composite for efficient adsorption of ciprofloxacin in fresh and saline solutions

Hanaa L. Essa [a,b,1], Hebatullah H. Farghal [a,1], Tarek M. Madkour [a], Mayyada M.H. El-Sayed [a,*]

[a] Department of Chemistry, School of Sciences and Engineering, The American University in Cairo, Cairo, 11835, Egypt
[b] Pesticides Phytotoxicity Department, Central Agricultural Pesticides Lab, Agricultural Research Center, Dokki, Giza, 12627, Egypt

ARTICLE INFO

Keywords:
Bentonite clay
Intercalation
Ciprofloxacin HCl
Contaminants of emerging concern
Chitosan
Wastewater treatment
SDGs 6 and 12

ABSTRACT

In alignment with the sustainable development goals (SDGs), recent trends in water management have been directed toward using environmentally friendly bio-based materials for removing contaminants. In this work, we prepared a biocomposite of chitosan (CS) intercalated into acid activated calcium bentonite (Bent). A thermally stable mesoporous CS-Bent composite was prepared with a zeta potential of 15.5 to −34.4 mV in the pH range of 2.22–10. The biocomposite successfully removed up to 99.2% and 50 mg/g of the antibiotic ciprofloxacin HCl (CPX) at pH 5.5 via electrostatic and hydrogen bonding forces. In a multi-component aqueous system of heavy metal and CPX, the composite was more selective to CPX than to the heavy metals and removal of CPX in this system was comparable to that in a single-component system. The composite also maintained its high adsorption efficiency in NaCl solutions which makes it suitable for treating fresh and saline solutions. The combination of CS and bent produced a biodegradable eco-friendly composite characterized with good thermal and surface properties along with efficient and selective adsorption performance.

1. Introduction

Contaminants of emerging concern are a newly discovered group of contaminants which are present at minute concentrations and could pose health risks over prolonged exposure times. There is no well-established regulatory framework that controls their release limits in the environment. They persist in the environment and have the potential to alter the physiology of living organisms. The most important classes are pharmaceuticals and personal care products, disinfectants, flame retardants, pesticides, .etc [1]. One of the emerging contaminants that are frequently used is the Ciprofloxacin HCl (CPX) which is one of the fluoroquinolone antibiotics that are extensively prescribed against bacterial infections such as sexually transmitted diseases and urinary tract infections [2,3]. A concentration of 14 mg/L was detected in the effluents of a local wastewater treatment plant in India [4], while concentrations of up to 28–30 mg/L were also reported in industrial wastewater effluents in India [5].

Several methods have been applied for the eradication of emerging contaminants from wastewater such as membrane filtration [6], advanced oxidation processes and ozonation [7]. Among the effective and potentially economical techniques, adsorption is distinguished by its facile operation, ease of reusing the adsorbents, and diversity in the type of adsorbents that can be utilized. Because of

* Corresponding author.
E-mail address: mayyada@aucegypt.edu (M.M.H. El-Sayed).
[1] Authors equally contribute to the published work.

https://doi.org/10.1016/j.heliyon.2024.e28641
Received 1 July 2023; Received in revised form 25 January 2024; Accepted 21 March 2024
Available online 23 March 2024

their large surface area and porosity, clays have been extensively regarded as effective adsorbents. Well-known classes of clays encompass smectites, pylophyllite, bentonite, Fuller's earth, kaolinite, sepiolite in addition to vermiculite, among others [8]. Bentonite – the one used in this study - is an aluminum phyllosilicate consisting mainly of montmorillonite (MMT) (80–90% by weight). Bentonites are classified into swelling (sodium bentonite) and non-swelling (calcium bentonite) [9]. The clay structure consists of layers, each formed of two types of structural sheets, where each two octahedral silica sheets hold one tetrahedral aluminum sheet in between. Due to the cationic substitution within the layers, such as replacing Si^{4+} by Al^{3+} in the tetrahedral sheet, or Al^{3+} by Fe^{2+} or Mg^{2+} in the octahedral sheet, the clay layers acquire negativity that is balanced by the charge of the interchangeable positive ions like Na^{+}, K^{+}, Ca^{2+}in the interlayer together with water molecules that are held by ion-dipole forces. Therefore, the chemical structure of bentonite has the empirical formula $\mathbf{[\,(Si^{Al})_4\,(Al^{Fe.\,Mg})_2\,O_{10}\,(OH)_2\,]_2 \bullet Mn \bullet mH_2O}$ [9–11].

Various reports studied the adsorption of CPX with clay. Calcined bentonite successfully adsorbed CPX from water with a maximum adsorption capacity (q_m) of 114.4 mg/g at 25 °C [12]. Also, silica and iron pillared clays were capable of removing CPX at q_m 100.6 and 122.1 mg/g at 20 °C, respectively [13]. Bentonite clay was incorporated with biochar in a composite to remove CPX from water and yielded a q_m of 190 mg/g at pH 6 [14].

Bentonites have been subjected to several modifications to enhance their surface area for targeted applications. These include the integration of glucosylated dendrimers into bentonite clays forming a microporous structure that improves their capability for water treatment [15]. Also, bentonite was intercalated with the linear polysaccharide chitosan for the elimination of ammonium nitrogen from water [16]. Additional modification was performed when chitosan (CS) was crosslinked with epichlorohydrin to form a composite with bentonite for the elimination of Ni(II) and Cd(II) from water [17]. Another composite of magnetic chitosan grafted on graphene oxide was capable of adsorbing CPX at a q_m of 282.5 mg/g at pH 5 [18].

Thus, this current study investigates the modification of clay to increase its surface area and enhance its physicochemical properties through its thermal acid activation followed by its intercalation with chitosan biopolymer for the removal of CPX from aqueous solutions. The incorporation of chitosan should improve the biodegradability properties of the composite while the clay could act as an immobilization material for chitosan to increase the composite's mechanical strength [19,20].

2. Materials and methods

2.1. Materials

Calcium bentonite was purchased from International Company for Mining & Investments ECC, Egypt. The analysis of the clay composition by Wavelength Dispersive X-Ray Fluorescence Spectrometry (XRF) (Axios advanced, Sequential WD_XRF Spectrometer, PANalytical 2005) is given in Table S1. Sulfuric acid 98% was purchased from Penta, Prague, Czech Republic, and acetic acid was purchased from advent, India, while high MW chitosan (MW 310–375 kDa, 75% degree of deacetylation) was brought from Sigma Aldrich, Iceland. For adsorption, Ciprofloxacin hydrochloride (CPX) of purity above 99.6 % was supplied from Shangya Jingxin Pharma, China. The empirical formula of CPX is $C_{17}H_{18}FN_3O_3HCl{\cdot}H_2O$ and its MW is 367.8 g/mol. Lead acetate trihydrate (purity 99%) was obtained from El-Nasr company for chemical industries (Adwic), Egypt, while zinc sulfate heptahydrate (purity 98%) and copper acetate monohydrate (purity 99%) were purchased from Piochem, Egypt. NaCl (purity ≥99.5%) was obtained from Fisher Scientific, Loughborough, UK. Methanol was purchased from Brand Chemicals, Egypt.

2.2. Preparation of acid activated bentonite (bent)

Pristine calcium bentonite was heated in the oven at 80 °C for 6h to get rid of any moisture. The cation exchange capacity (CEC) of the thermally treated clay (denoted here by B) was estimated to be 28 ± 2.8 meq/100 g as per the method described in the SI along with Fig. S1. B was soaked in 10 times its weight sulfuric acid inside a 50 mL round bottom flask and refluxed in an oil bath for 4h at 90 °C. Then, the suspension was filtered (Double Rings filter paper 102) and rinsed with deionized water till the activated bentonite (Bent) acquired a neutral pH [21]. Two activation parameters were investigated to determine the optimal conditions for CPX removal through varying the acid concentration (2 M, 4 M, 6 M) and contact time of soaking (1h, 2h, 4h). The optimal conditions were 6 M and 4h, respectively (Fig. S2 of SI).

2.3. Preparation of biopolymer (CS)/bentonite composite (CS-Bent)

A mass of 0.25 g of the intercalating agent CS was dissolved in 1% acetic acid and then placed into a conical flask containing 1g of Bent previously suspended in 100 mL of deionized water and stirred for 15 min then sonicated for another 15 min at room temperature 25 ± 2 °C. Hereafter, this mixture was agitated for 2 h at 1500 rpm and 25 ± 2 °C. The suspension was centrifuged at 5000 rpm and the collected pellet was rinsed with deionized water to get rid of the excess of the intercalating agent and dried in the oven at 70 °C overnight. The resulting solid chitosan-bentonite (CS-Bent) composite was kept in the desiccator for further application.

2.4. Characterization

To determine surface charge of Bent or CS-Bent at different pHs, zeta potential measurements (Malvern zeta sizer, Nano Zs, Malvern, UK) were performed after dissolving a mass of 15 mg of Bent or CS-Bent composite in 100 mL of deionized water and sonicating for 15 min, then distributing the suspension over five different falcon tubes for pH adjustment using either dilute HCl or

NaOH solutions. FTIR measurements (Thermo Scientific, Nicolet 380 FTIR spectrometer) were carried out on Bent, and CS-Bent composite to determine their main functional groups using KBr pellet method in the range of 4000 to 500 cm^{-1}. To investigate the thermal stability, TGA (Lab Tron LTGA-A10, England) was applied on 20–35 mg of Bent or CS-Bent at a temperature range of 25–800 °C. SEM (ZEISS- LEO SUPRA 55, Jena, Germany) was used to investigate the morphology of Bent and CS-Bent composite after gold sputtering (ANATECH HUMMER™ 8.0, USA) for 3 min at 15 mA. The elemental composition of Bent and CS-Bent composite was determined using EDX (JEOL, JCM 6000 plus, Akishima, Tokyo, Japan), at 15 KV and a working distance of 19 mm. XRD with Cu Kα radiation (Bruker D8 Discover, USA) at 1.54 A^0 was used to determine the phase and constitution of B, Bent, and CS-Bent which were precipitated on a silicon holder. The specific surface area was obtained using a BET surface area analyzer (ASAP 2020) after degassing the samples at 100 °C below 10^{-4} bar for 4h to remove any moisture and other contaminants.

2.5. Adsorption and regeneration

Batch adsorption was carried out using a rotary shaker at 60 rpm and room temperature (25 °C ± 2). Screening studies on B, Bent, and CS-Bent were first performed using an adsorbent dose of 1.067 g/L and initial concentration of 50 ppm of CPX at pH 5.5. The effect of contact time on CPX adsorption onto CS-Bent was performed within a time interval of 10–240 min using three initial CPX concentrations of 25, 50, and 75 ppm at an adsorbent dose of 1.067 g/L and pH 5.5. Also, the effect of initial concentration was investigated in the range of 10–50 ppm using an adsorbent dose of 1.067 g/L at pH 5.5. In addition, the effect of adsorbent dose was carried out in the range of 0.267–4.26 g/L at an initial concentration of 50 ppm and pH 5.5. After adsorption, the adsorbent was separated by ultracentrifugation at 8000 rpm for 5 min and the supernatant was measured spectrophotometrically (Pg instruments, T80+ spectrometer) at 274 nm. The percent removal and the adsorption capacity were calculated according to Eqs. 2 and 3 in the SI. To predict the kinetic profiles, the pseudo-first order (Eq. 4, SI), pseudo-second order (Eq. 5, SI) and intra-particle diffusion (Eq. 6, SI) models were applied. To predict the equilibrium isotherms, Langmuir (Eq. 7, SI) and Freundlich (Eq. 8, SI) models were applied. The effect of salinity was also studied where 0.75, 1.5, and 3 g% of NaCl were added to 25 ppm CPX solution and compared to a CPX solution with no salt. Besides, the selectivity of the composite for CPX was tested in a multi-component aqueous solution containing the heavy metals of Pb(II), Zn(II), and Cu(II), each at an initial concentration of 25 ppm along with 25 ppm CPX, and adsorption was conducted at pH 5.5. In the single-component system, the initial concentrations of CPX and each of the heavy metals were prepared by diluting aqueous

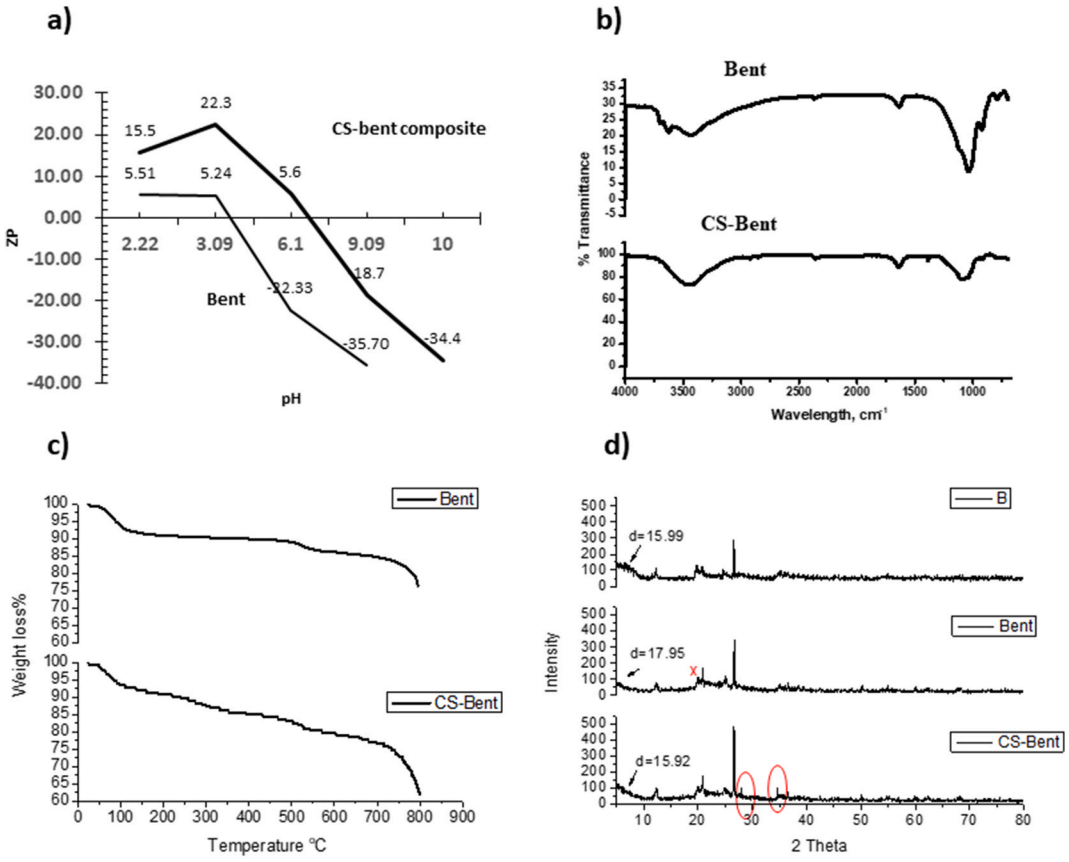

Fig. 1. Zeta potential of Bent and CS-Bent composite (a), FTIR spectra of Bent and CS-Bent composite (b), TGA of Bent and CS-bent composite (c), and XRD of B, Bent, and CS-Bent (d).

stock solutions of 1000 ppm of each contaminant where 2.5 mL of each stock solution was diluted to 100 mL with water to obtain 25 ppm. For the quaternary system, 2.5 mL of each stock solution were all added to a single 100-mL volumetric flask then completing to the mark with water. The concentrations of the heavy metals were detected using Inductively Coupled Plasma (ICAP™ 7400 Duo, Bremen, Germany) at wavelengths of 283, 334, and 224 nm for Pb(II), Zn(II), and Cu(II), respectively, after constructing a calibration curve for each of the heavy metals.

Regeneration of CS-Bent was performed after running an adsorption experiment at an adsorbent dose of 1.067 g/L, initial CPX concentration of 25 ppm and pH 5.5 for 30 min. Then, desorption of CPX was performed using 50 mL of 0.1 N NaOH for 20 min followed by deionized water for 10 min or using 50 mL methanol for 30 min. Regeneration was done for two consecutive cycles.

3. Results and discussion

In what follows, three materials will be investigated, the thermally treated clay (B), acid activated clay (Bent), and (chitosan/acid activated clay composite (CS-Bent).

3.1. Characterization

Fig. 1a demonstrates zeta potential measurements of Bent and CS-Bent composite which exhibited values of 5.51 to −35.70 and 15.5 to −34.4 mV at the working pH range of 2.22–10 and 2.5–10.7, respectively, indicating that the composite is positively charged at acidic pHs and negatively charged at basic pHs. In this study, we chose pH 5.5 as the working pH to impart an almost neutral charge on the composite and thus enhance its adsorption properties with the positively charged CPX at this pH since in acidic media, both the composite and CPX have positive charges while in basic media both the composite and the CPX have negative charges, leading to repulsion forces that hinder the adsorption. As shown in Fig. 1a, CS-Bent is more positive than Bent across the whole investigated pH range, inferring the possibility of a physical interaction occurring between the slightly positive to neutral composite and the positively charged CPX at pH 5.5.

The FTIR spectrum of Bent shown in Fig. 1b has characteristic peaks at 3621, 3436, 1685, 1121, 950, and 750 cm^{-1} for the Al–OH–Al bond, water molecules in the interlayer spaces, annular deformation of the water molecules, Si=O of the tetrahedral sheet, bending Al═Al═OH and Fe═OH═Mg, respectively; while the spectrum of CS-Bent composite shows a peak at about 3200 cm^{-1} assigned to NH of the amine group of chitosan which overlapped with the 3400 cm^{-1} band assigned to the OH group of Bent to give a broad band. This overlap possibly indicates a hydrogen bonding that can take place between the NH or OH groups in chitosan and the OH groups in bentonite [22]. The peak at 2950-2850 cm^{-1} corresponds to the aliphatic CH stretching in the chitosan skeleton and the band at 1638 cm^{-1} is ascribed to the NH bending. These results are in accordance with findings reported in previous literature [17,23,24]. Thermogravimetric analysis of Bent and CS-Bent composite are shown in Fig. 1c. The 6.71% weight loss of Bent at 0–110°C is due to the elimination of interlayer H_2O molecules. Constant weight loss in the range of 200–450 °C is observed owing to the dehydration of interlayer cations upon heating, and a final weight loss of Bent to 77% of its weight occurs at 800 °C as displayed on the graph. On the other hand, the composite exhibits similar weight losses as Bent. In addition, it encounters a 10 % weight loss in the range of 200–300 °C owing to the chitosan deacetylation, then another weight loss in the region of 300–480 °C attributed to the breakdown of the backbone chain and the decomposition of the organic compound [25].

Fig. 1d shows the XRD patterns of B, Bent, and CS-Bent. For B, the XRD pattern confirms the presence of smectite and quartz minerals at the positions of 5.57, 12.32, 19.73, 20.81, 24.83, 26.57, and 61.25°, and the d basal space of the peak at 5.57° is 15.99 nm which agrees with a previous study [26]. This peak was shifted to 5.72° after the acid activation step to give a d spacing of 17.95 nm for Bent, and this confirms the increase in the spaces within clay layers by acid activation. The peak of B at 19.73° decreased in intensity after acid treatment – marked on the XRD graph as X - because smectite was affected by the acid treatment [26]. Regarding the XRD of CS-Bent, the signals at 27.92° and 35.03° – denoted by red circles - confirm the intercalation of chitosan between the interlayer spaces of clay since the d basal space shrank to 15.92 nm again after shifting of the peak to 5.48° [27].

Table 1 shows the elemental analysis of B, Bent, and CS-Bent, which reveals that the clay composition in terms of the ratio of Si/Al increased from 2:1 in B to 4.9 and 4.4 in Bent and CS-Bent, respectively, due to the leaching of aluminum ions and other metal cations after thermal treatment and acid activation [21]. In addition, the presence of carbon atoms in CS-Bent composite indicates the successful incorporation of chitosan in the clay structure, whereas the absence of Ca cations in CS-Bent resulted from the exchange of Ca with chitosan in the interlayer spaces. Also, the oxygen percentage increased in CS-Bent relative to Bent because of the OH groups of chitosan.

The morphologies of Bent and CS-Bent were investigated by SEM at a magnification of 10000 as depicted in Fig. 2. No clear change in the surface morphology of Bent (Fig. 2a) can be observed after compositing with chitosan (Fig. 2b) since intercalation occurs between the clay layers. Also, a photograph of the composite is given in Fig. 2c.

Table 1
Elemental analysis of B, Bent, and CS-Bent composite.

Material	O%	Si%	Al%	Fe%	Ca%	C%
B	57.33	20.74	9.93	7.24	0.79	–
Bent	47.65	42.59	8.57	0.47	0.16	–
CS-Bent	53.15	33.41	7.51	0.63	–	3.67

Table 2 shows the surface area and porosity parameters for B, Bent, and CS-Bent. Clearly, the BET surface area of B increased after acid activation by about 71% to form Bent indicating the formation of new pores after the octahedral cation exchange with H^+ leading to the increase in surface area. However, on adding chitosan the surface area decreased again by about 20% relative to Bent indicating the blockage of pores after incorporation of chitosan [28]. The same trend was observed for the Langmuir surface areas. Also, the pore volume increased by 93% in Bent relative to B and decreased again in the CS-Bent composite by 28% for the same reason alluded to earlier. Comparable pore sizes in the range of 2–50 nm for all three clays indicate a mesoporous structure. The pore volume distribution curves provided further confirmation (Fig. S3) that show most pore sizes laying in the range below 20 nm.

The above observations of the behavior of the microstructures could be explained taking into consideration the confinement of the polymer chains within the layers of the clay. In the absence of constraints such as fillers, strain-induced crystallites, etc. [29], polymeric chains are free to move in the bulk state. However, reducing the free volume accessible by these chains reduces the configurational entropy of the polymeric samples as the confinement of the polymeric chains within a smaller and smaller volume restricts its molecular dynamics. The effect is even more pronounced due to the adsorption of the polymer chains on the surface of the clay layers, which causes the polymeric chains to be extended or contracted and thus impacting its elastic behavior. The results clearly manifest that the intercalation of the chitosan polymer within the layers of the clay limited the conformational changes of the polymeric chains causing the chains to acquire more flattened and extended configurations, leading to "strain amplifications" [30]. As the chains confined in different spaces interconnect through hydrogen bonding, a second physical network is formed, leading to the observed behavior, otherwise known as "filler networking" [31]. Interestingly, previous studies are in excellent agreement with these observed findings [32].

3.2. Adsorption studies

Fig. 3 shows the removal efficiency of the adsorbents B, Bent, and CS-Bent at a dose of 1.067 g/L with 50 ppm CPX at pH 5.5. Clearly, the three adsorbents show comparable removal efficiencies ranging between 90 and 97%. CS-Bent was chosen in this study as it combines the eco-friendly properties of the biodegradable and functional chitosan along with the surface characteristics of clay. In addition, the introduction of a polymer into the structure of clay improved the handling and processing properties of clay. The pH applied in this study is 5.5, at which the composite exhibits a neutral charge that can possibly bind with the positively charged CPX (pK_a 6.0 and 8.8 [33]) through physical forces of van der Waals or hydrogen bonding. Below this pH, the composite is positively charged leading to electrostatic repulsion with the positively charged CPX while above this pH, the composite is negatively charged resulting in electrostatic repulsion with the negative CPX. B and Bent, on the other hand, exhibited comparable removal efficiencies to that of CS-Bent since they are negatively charged at pH 5.5 and hence can still bind to the positively charged CPX through physical interactions that can involve electrostatic attraction or hydrogen bonding. Although the surface area and pore volume of CS-Bent are smaller than their Bent counterparts (Table 2) likely since CS blocked some of the pores of Bent, the removal efficiencies of Bent and CS-Bent are comparable. The reduction of surface area and pore volume was compensated for with the addition of the OH and NH functional groups of CS which bind to CPX via electrostatic and hydrogen bonding forces.

Fig. 4a shows the time profiles for the adsorption of CPX on 1.067 g/L CS-Bent at three different initial concentrations, *i.e.,* 25, 50, and 75 ppm. It is evident from the figure that equilibrium is reached at about 20, 40, and 60 min for the respective three concentrations, achieving q_e values of about 23, 42, and 42 mg/g. Previous literature on the adsorption of CPX on montmorillonite reported an equilibrium time of 1h on applying an initial concentration of 250 ppm at an adsorbent dose of 2 g/L [34]. Also, the adsorption of CPX on biochar-bentonite composite reached equilibrium at 1h on applying an initial concentration of 25 ppm at an adsorption dose of 1 g/L [14].

To better understand the adsorption behavior, kinetic modeling was performed on the profiles obtained at 50 ppm using pseudo-first order, pseudo-second order, and intra-particle diffusion models (Fig. S4 of SI). As shown in Table 3, kinetics followed the pseudo-second order model as inferred from its higher R^2 value and lower *RMSE* relative to the pseudo-first order model. Also, q_e was well predicted from this model (41.67 mg/g) and was in alignment with the experimental value (42.03 mg/g). The intra-particle diffusion linear plot (Fig. S4c) showed two stages, the first stage indicates that adsorption rate is controlled by pore diffusion with no film diffusion limitations, while the second stage represents equilibrium [35].

The adsorption of CPX was conducted at different initial concentrations using 1.067 g/L of CS-Bent as depicted in Fig. 4b which

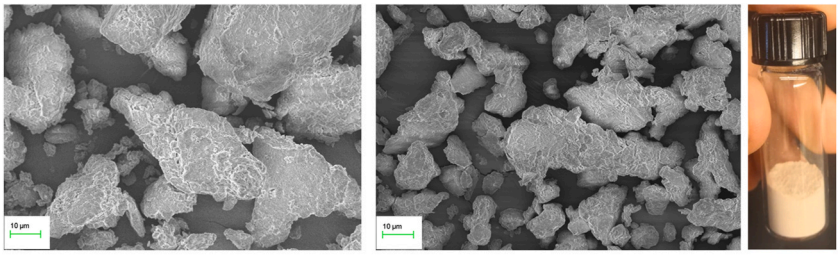

Fig. 2. SEM images of Bent (a) and CS-bent (b), and a photograph of the CS-Bent composite (c).

Table 2
Surface areas and pore volumes of B, Bent and CS-Bent.

Material	BET Surface area ($m^2.g^{-1}$)	Pore volume (cm^3)	Langmuir surface area ($m^2.g^{-1}$)	Pore size (nm)
B	60.29	0.0782	87.31	6.08
Bent	209.13	1.0624	303.69	6.67
CS-Bent	167.46	0.7650	242.97	6.88

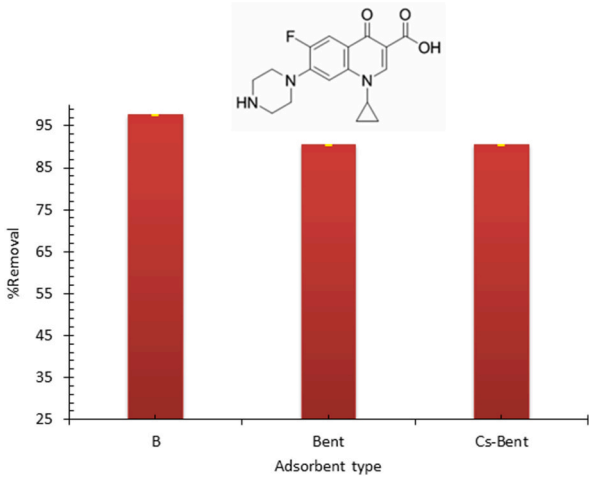

Fig. 3. %Removal of CPX by B, Bent, and CS-Bent at an initial concentration of 50 ppm, pH 5.5, adsorbent dose of 1.067 g/L and room temperature (25 ± 2 °C). The embedded image shows the chemical structure of ciprofloxacin.

reveals that the equilibrium adsorption capacity increases gradually from about 9 to 42 mg/g, while the percent removal decreases slightly from about 97 to 91% as the initial concentration increases from 10 to 50 ppm. Similar findings have been reported regarding the adsorption of CPX onto multi-walled carbon nanotubes. This behavior may be attributable to the increased mass transfer rate brought about by the increase in concentration gradient [36].

The equilibrium adsorption isotherms of CPX onto CS-Bent are displayed in Fig. 4c. As shown, q_e vs C_e profile is L-shaped indicating monolayer coverage. This was further confirmed by fitting the isotherm to Langmuir and Freundlich models where the former showed higher R^2 value. Also, the predicted q_m is in agreement with the experimental value (Table 4). This suggests that adsorption occurred at homogenous energetically equivalent sites. CPX adsorption on HCl-activated bentonite also followed Langmuir isotherm with q_m of 305.2 mg/g at pH 5.5 [37].

Fig. 4d shows the study of CS-Bent dose effect on the adsorption of 50 ppm CPX. It can be observed that q_e decreases gradually from about 59 to 11 mg/g while percent removal increases from about 31 to 99% on increasing the dose from 0.267 to 4.26 g/L. The adsorption capacity decreased probably due to agglomeration of CS-Bent particles and consequent overlapping of active sites, while the percent removal increased due to the increase in the available adsorption sites [38].

Fig. 4e shows the regeneration of CS-Bent after two adsorption/desorption cycles, where the percent removal of CPX decreased by about 65% and 21% in the second cycle when applying 0.1 N NaOH or methanol as desorbing agents, respectively. Thus, this adsorbent could be better regenerated by methanol probably since methanol is less harsh on the structure of chitosan than NaOH as it has been reported that NaOH deacetylates chitosan [39]. After the exhaustion of the adsorbent, it can be utilized for energy recovery by incineration in municipal solid waste plants [40], or it can be applied as a coating for the controlled release of phosphorous fertilizers in soil and water while being biodegradable in soil [41], or reused as a catalyst to produce biofuels from waste cooking oils [42].

4. Mechanism of adsorption

The FTIR spectra of CS-Bent prior and post CPX adsorption (Fig. 5) demonstrate a shift in the OH or NH band of the adsorbent from 3466 before adsorption to 3460 cm^{-1} after adsorption, besides a clear change in the intensity which could be assigned to the hydrogen bonding between the OH or NH of the composite and CPX functional groups. Other mechanisms could possibly occur such as van der Waals interactions between the neutral CS-Bent and the positively charged CPX [43]. A further confirmation for CPX adsorption was done by measuring the zeta potential of the adsorbent before and after adsorption. It was found that the zeta potential changed from -5.9 ± 2.9 to -2.62 ± 0.717, which could be attributed to the presence of the positively charged CPX which increased the positivity of the adsorbent.

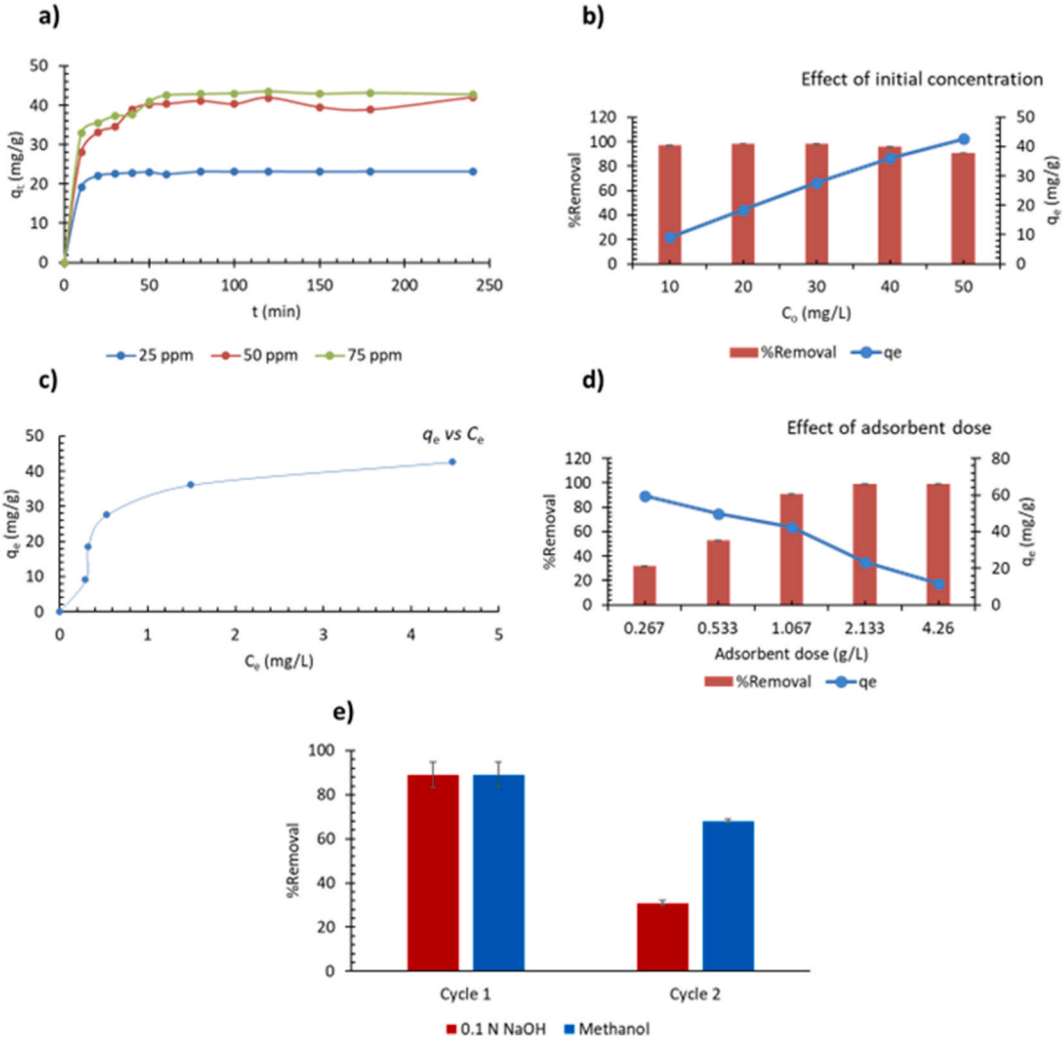

Fig. 4. Adsorption time profiles of CPX on 1.067 g/L CS-Bent at initial concentrations of 25, 50, and 75 ppm at pH 5.5 and room temperature (25 ± 2 °C) (a), Adsorption capacities and removal efficiencies at different initial concentrations of CPX, at 1.067 g/L and pH 5.5 (b), Adsorption isotherm at pH 5.5 and 25 ± 2 °C (c), Effect of adsorbent dose on the adsorption of 50 ppm CPX at pH 5.5 (d), and regeneration study after adsorption of CPX on CS-Bent using an adsorbent dose of 1.067 g/L, initial concentration of 25 ppm and pH 5.5 (e).

Table 3
Kinetic modeling parameters predicted for the adsorption of 50 ppm CPX on CS-Bent.

Pseudo-first order				Pseudo-second order				Intra-particle diffusion		
$q_{e,}$ mg/g	$k_{1,}$ min^{-1}	R^2	RMSE	$q_{e,}$ mg/g	k_2 $g.mg^{-1}.min^{-1}$	R^2	RMSE	C	k_{id} $mg.g^{-1}.min^{-0.5}$	R^2
2.12	0.011	0.2409	0.654	41.67	0.006	0.9967	0.087	0	6.39	0.9825

Table 4
Parameters for equilibrium adsorption isotherms of CPX on CS-Bent at pH 5.5 and 25±2°C.

Langmuir isotherm			Freundlich isotherm		
q_m (mg/g)	k_d (L/mg)	R^2	K_f (mg/g)(L/mg)^n	1/n	R^2
50.51	0.758	0.9607	25.832	0.4509	0.7073

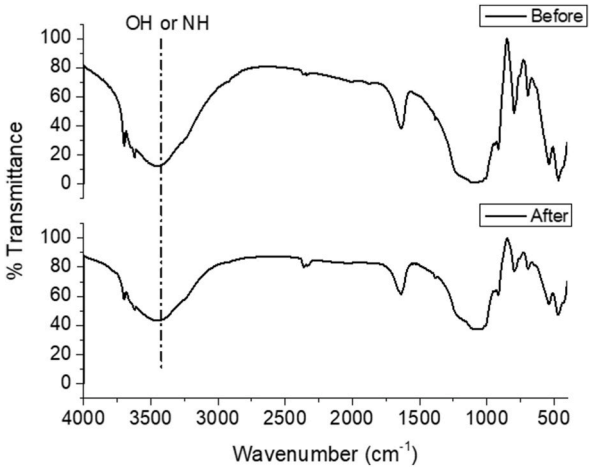

Fig. 5. FTIR spectra of CS-Bent before and after adsorption of CPX at an initial concentration of 25 ppm and adsorbent dose of 1.067 g/L at pH 5.5.

5. Effect of salinity and competing heavy metals

The effect of salinity on the adsorption of CPX on CS-Bent was studied using three NaCl concentrations of 0.75, 1.5, and 3 g/100 mL as shown in Fig. 6a. It is evident that the addition of NaCl did not appreciably affect the removal of CPX by CS-Bent since the removal percentage decreased by only about a maximum of 15% at the highest NaCl concentration of 3 g/100 mL which mimics the sea or ocean water. This reduction in removal could be assigned to the competition between CPX and NaCl on the adsorbent sites [43]. This confirms the selectivity of the adsorbent towards CPX and its potential applicability in saline conditions. The combination of chitosan and bentonite imparted an overall neutral charge to the composite at the studied pH which favors physical interactions like van der Waals to occur. Thus, the shielding action of NaCl is diminished owing to the overall neutrality of the composite [44]. To examine the stability of the composite in saline conditions, the composite was weighed before and after adsorption it showed an increase in weight by 5.66% that is equivalent to the amount of CPX adsorbed, thus indicating the stability of the composite.

The effect of competing heavy metals Pb(II), Zn(II), and Cu(II) on the adsorption of CPX onto CS-Bent was investigated as shown in Fig. 6b. The removal of heavy metals in the quaternary system decreased significantly by about 37%, 40%, and 13%, respectively, relative to their single systems. However, CPX removal efficiency decreased slightly by about 9% in the quaternary system as compared to the single system which confirms that the adsorbent is more selective to CPX than to the heavy metals. This could be owed to the abundance of OH and NH groups on chitosan and OH groups on Bent, which facilitated hydrogen bonding between CPX and CS-Bent. On the other hand, it is anticipated that the heavy metals bind to the composite through inner-sphere or outer-sphere complexation with the amine group of chitosan [45]. The chemical short-range nature of the complexation interaction makes it less competitive relative to the hydrogen bonding. Pb(II) exhibited the highest removal in the single system by virtue of its higher energy of hydration and smaller hydrated radius relative to Zn(II) and Cu(II) which results in higher charge density. This result is consistent with previous findings reported for the adsorption of these heavy metals on the mineral based adsorbent fly ash [46]. In the multi-component system, Pb(II) showed less removal relative to the single system but still higher than Zn(II) and comparable to Cu(II). The presence of other heavy metals with Pb(II) may have hindered its diffusion through the adsorbent pores, especially that these heavy metals have larger hydrated spheres than Pb(II) which may cause steric hindrance.

6. Comparison with literature

In comparison to other adsorbents previously reported, the maximum adsorption capacity of CS-Bent is better than clay based adsorbents, however, it is less than biochar-clay adsorbents since biochar is known for its high adsorption capacity (Table 5) [47].

7. Conclusion

This work shows successful intercalation of clay with chitosan for the preparation of an environmentally friendly composite capable of adsorbing CPX from fresh and saline solutions. The incorporation of chitosan into clay was confirmed by FTIR and XRD measurements. The formed composite was mesoporous and thermally stable, with an almost neutral charge at pH 5.5 which allowed it to adsorb the positively charged CPX via physical interactions as confirmed by the FTIR before and after adsorption. Adsorption equilibrium followed Langmuir isotherm model with q_m of about 50 mg/g, while kinetics followed the pseudo-second order model and the intra-particle diffusion model which showed that pore diffusion is the rate determining step. The composite was regenerated with methanol and lost about 20% of its removal in the second cycle; thus, it is recommended to dispose of the adsorbent after two cycles because it is non-hazardous to the environment and biodegradable. The composite showed high selectivity to CPX in saline solutions of NaCl that mimicked the sea or ocean water, and in muti-component solutions with competing heavy metals of Pb(II), Zn(II), and Cu(II).

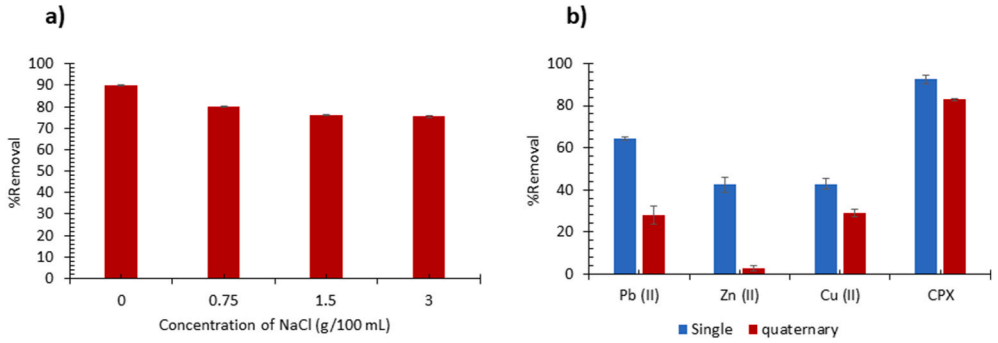

Fig. 6. Adsorption of 25 ppm CPX on 1.067 g/L CS-Bent at pH 5.5 under different concentrations of NaCl (a), and in a multi-component system of heavy metals (b).

Table 5
Comparison of CS-Bent maximum adsorption capacity for CPX to those of other clay adsorbents reported in literature.

Adsorbent	q_m (mg/g) pH Temperature °C	Ref.
Modified montmorillonite	5.1 (Langmuir) – 25	[48]
Montmorillonite	1.9 (Langmuir) – 25	[48]
Al-pillared clays	17.78 (Sips) 10 20	[13]
Municipal solid waste biochar-Montmorillonite	167.36 (Hills) 5–6 25	[47]
Illite (IMt-2) clay	33 (Langmuir) 4–5.5 –	[49]
CS-Bent	50.5 (Langmuir) 5.5 25	This study

Funding

This work was supported by USAID ASHA Grant Number: AID-ASHA-G-17-00010 for providing lab equipment, and by the American University in Cairo intramural grant: SSE-CHEM-M.E-FY17-RG-2019-Feb-28-21-44-19.

CRediT authorship contribution statement

Hanaa L. Essa: Conceptualization, Formal analysis, Investigation, Writing – original draft. **Hebatullah H. Farghal:** Conceptualization, Formal analysis, Investigation, Writing – original draft. **Tarek M. Madkour:** Conceptualization, Funding acquisition, Supervision, Writing – review & editing. **Mayyada M.H. El-Sayed:** Conceptualization, Funding acquisition, Methodology, Supervision, Writing – review & editing.

Declaration of competing interest

The authors declare that they have no known competing financial interests or personal relationships that could have appeared to influence the work reported in this paper.

Appendix A. Supplementary data

Supplementary data to this article can be found online at https://doi.org/10.1016/j.heliyon.2024.e28641.

References

[1] P.R. Rout, et al., Treatment technologies for emerging contaminants in wastewater treatment plants: a review, Sci. Total Environ. 753 (2021) 141990.
[2] M. Ramesh, et al., Responses of Cirrhinus mrigala to second-generation fluoroquinolone (ciprofloxacin) toxicity: assessment of antioxidants, tissue morphology, and inorganic ions, Environ. Toxicol. 36 (5) (2021) 887–902.
[3] T. Thai, B.H. Salisbury, P.M. Zito, Ciprofloxacin, in: StatPearls, StatPearls Publishing, 2021 [Internet].
[4] J. Fick, et al., Contamination of surface, ground, and drinking water from pharmaceutical production, Environ. Toxicol. Chem. 28 (12) (2009) 2522–2527.
[5] P.K. Mutiyar, A.K. Mittal, Risk assessment of antibiotic residues in different water matrices in India: key issues and challenges, Environ. Sci. Pollut. Control Ser. 21 (2014) 7723–7736.
[6] S. Kim, et al., Removal of contaminants of emerging concern by membranes in water and wastewater: a review, Chem. Eng. J. 335 (2018) 896–914.
[7] L. Rizzo, et al., Consolidated vs new advanced treatment methods for the removal of contaminants of emerging concern from urban wastewater, Sci. Total Environ. 655 (2019) 986–1008.
[8] E.C. Lima, Removal of emerging contaminants from the environment by adsorption, Ecotoxicol. Environ. Saf. 150 (2018) 1–17.
[9] A. Ahmed, et al., Studies on the mineral and chemical characteristics of Pindiga bentonitic clay, Petroleum Technology Development Journal 1 (1) (2012) 56–63.
[10] F. Rodríguez, et al., Characterization of cetylpyridinium bromide-modified montmorillonite incorporated cellulose acetate nanocomposite films, J. Mater. Sci. 50 (10) (2015) 3772–3780.
[11] Y. Xi, R.L. Frost, H. He, Modification of the surfaces of Wyoming montmorillonite by the cationic surfactants alkyl trimethyl, dialkyl dimethyl, and trialkyl methyl ammonium bromides, J. Colloid Interface Sci. 305 (1) (2007) 150–158.
[12] R. Antonelli, et al., Adsorption of ciprofloxacin onto thermally modified bentonite clay: experimental design, characterization, and adsorbent regeneration, J. Environ. Chem. Eng. 8 (6) (2020) 104553.
[13] M.E. Roca Jalil, M. Baschini, K. Sapag, Removal of ciprofloxacin from aqueous solutions using pillared clays, Materials 10 (12) (2017) 1345.
[14] A. Ashiq, et al., Municipal solid waste biochar-bentonite composite for the removal of antibiotic ciprofloxacin from aqueous media, J. Environ. Manag. 236 (2019) 428–435.
[15] S. Nousir, et al., Improved carbon dioxide storage over clay-supported perhydroxylated glucodendrimer, Can. J. Chem. 95 (9) (2017) 999–1007.
[16] P. Haseena, et al., Adsorption of ammonium nitrogen from aqueous systems using chitosan-bentonite film composite, Procedia Technology 24 (2016) 733–740.
[17] V.N. Tirtom, et al., Comparative adsorption of Ni (II) and Cd (II) ions on epichlorohydrin crosslinked chitosan–clay composite beads in aqueous solution, Chem. Eng. J. 197 (2012) 379–386.
[18] F. Wang, et al., Removal of ciprofloxacin from aqueous solution by a magnetic chitosan grafted graphene oxide composite, J. Mol. Liq. 222 (2016) 188–194.
[19] R. Ollier, E. Rodriguez, V. Alvarez, Unsaturated polyester/bentonite nanocomposites: influence of clay modification on final performance, Compos. Appl. Sci. Manuf. 48 (2013) 137–143.
[20] Q. Liu, et al., Adsorption of an anionic azo dye by cross-linked chitosan/bentonite composite, Int. J. Biol. Macromol. 72 (2015) 1129–1135.
[21] W. Wang, et al., Sulfuric acid modified bentonite as the support of tetraethylenepentamine for CO2 capture, Energy Fuels 27 (3) (2013) 1538–1546.
[22] X. Guo, et al., Preparation of chitosan-modified bentonite and its adsorption performance on tetracycline, ACS Omega 8 (22) (2023) 19455–19463.
[23] S. Biswas, et al., Application of chitosan-clay biocomposite beads for removal of heavy metal and dye from industrial effluent, Journal of Composites Science 4 (1) (2020) 16.
[24] H. Rafiei, M. Shirvani, O. Ogunseitan, Removal of lead from aqueous solutions by a poly (acrylic acid)/bentonite nanocomposite, Appl. Water Sci. 6 (4) (2016) 331–338.
[25] A. Kausar, et al., Preparation and characterization of chitosan/clay composite for direct Rose FRN dye removal from aqueous media: comparison of linear and non-linear regression methods, J. Mater. Res. Technol. 8 (1) (2019) 1161–1174.
[26] L. Zhirong, M.A. Uddin, S. Zhanxue, FT-IR and XRD analysis of natural Na-bentonite and Cu (II)-loaded Na-bentonite, Spectrochim. Acta Mol. Biomol. Spectrosc. 79 (5) (2011) 1013–1016.
[27] E.M. Azzam, S. Solyman, A.A. Abd-Elaal, Fabrication of chitosan/Ag-nanoparticles/clay nanocomposites for catalytic control on oxidative polymerization of aniline, Colloids Surf. A Physicochem. Eng. Asp. 510 (2016) 221–230.
[28] N. Horri, et al., Amine grafting of acid-activated bentonite for carbon dioxide capture, Appl. Clay Sci. 180 (2019) 105195.
[29] T.M. Madkour, J.E. Mark, Mesoscopic modeling of the polymerization, morphology, and crystallization of stereoblock and stereoregular polypropylenes, J. Polym. Sci. B Polym. Phys. 40 (9) (2002) 840–853.
[30] T.M. Madkour, S.K. Mohamed, A.M. Barakat, Interplay of the polymer stiffness and the permeability behavior of silane and siloxane polymers, Polymer 43 (2) (2002) 533–539.
[31] T. Madkour, J. Mark, Elastomeric properties of poly (dimethylsiloxane) networks having bimodal and trimodal distributions of network chain lengths, Macromol. Rep. 31 (1–2) (1994) 153–160.
[32] A. Nakatani, et al., Chain dimensions in polysilicate-filled poly (dimethyl siloxane), Polymer 42 (8) (2001) 3713–3722.
[33] U.E. Osonwa, et al., Enhancement of antibacterial activity of ciprofloxacin hydrochloride by complexation with sodium cholate, in: Bulletin of Faculty of Pharmacy, vol. 55, Cairo University, 2017, pp. 233–237, 2.
[34] B. Gulen, P. Demircivi, Adsorption properties of flouroquinolone type antibiotic ciprofloxacin into 2: 1 dioctahedral clay structure: Box-Behnken experimental design, J. Mol. Struct. 1206 (2020) 127659.
[35] H.H. Farghal, M. Nebsen, M.M.H. El-Sayed, Multifunctional chitosan/Xylan-Coated magnetite nanoparticles for the simultaneous adsorption of the emerging contaminants Pb(II), salicylic acid, and Congo red dye, Water 15 (4) (2023) 829.
[36] A. Avcı, İ. İnci, N. Baylan, Adsorption of ciprofloxacin hydrochloride on multiwall carbon nanotube, J. Mol. Struct. 1206 (2020) 127711.
[37] A. Maged, et al., Characterization of activated bentonite clay mineral and the mechanisms underlying its sorption for ciprofloxacin from aqueous solution, Environ. Sci. Pollut. Control Ser. 27 (26) (2020) 32980–32997.
[38] A. Rahdar, et al., Adsorption of ciprofloxacin from aqueous environment by using synthesized nanoceria, Ecological Chemistry and Engineering 26 (2) (2019) 299–311.
[39] E.A. Takara, J. Marchese, N.A. Ochoa, NaOH treatment of chitosan films: impact on macromolecular structure and film properties, Carbohydr. Polym. 132 (2015) 25–30.
[40] A. Wagner, et al., Incineration of nanoclay composites leads to byproducts with reduced cellular reactivity, Sci. Rep. 8 (1) (2018) 10709.
[41] E. Eddarai, et al., Chitosan-kaolinite clay composite as durable coating material for slow release NPK fertilizer, Int. J. Biol. Macromol. 195 (2022) 424–432.
[42] H.A. Ahmed, et al., Effect of reaction parameters on catalytic pyrolysis of waste cooking oil for production of sustainable biodiesel and biojet by functionalized montmorillonite/chitosan nanocomposites, ACS Omega 7 (5) (2022) 4585–4594.
[43] G. Gopal, C. Natarajan, A. Mukherjee, Adsorptive removal of fluoroquinolone antibiotics using green synthesized and highly efficient Fe clay cellulose-acrylamide beads, Environ. Technol. Innovat. 28 (2022) 102783.
[44] H.H. Farghal, M. Nebsen, M.M. El-Sayed, Exploitation of expired cellulose biopolymers as hydrochars for capturing emerging contaminants from water, RSC Adv. 13 (29) (2023) 19757–19769.
[45] K. Trimukhe, A. Varma, A morphological study of heavy metal complexes of chitosan and crosslinked chitosans by SEM and WAXRD, Carbohydr. Polym. 71 (4) (2008) 698–702.
[46] A.P. Caetano, et al., Unravelling the affinity of Alkali-activated fly ash cubic foams towards heavy metals sorption, Materials 15 (4) (2022) 1453.

[47] A. Ashiq, et al., Sorption process of municipal solid waste biochar-montmorillonite composite for ciprofloxacin removal in aqueous media, Chemosphere 236 (2019) 124384.
[48] A. Avcı, İ. İnci, N. Baylan, A comparative adsorption study with various adsorbents for the removal of ciprofloxacin hydrochloride from water, Water, Air, Soil Pollut. 230 (2019) 1–9.
[49] C.-J. Wang, Z. Li, W.-T. Jiang, Adsorption of ciprofloxacin on 2: 1 dioctahedral clay minerals, Appl. Clay Sci. 53 (4) (2011) 723–728.